Imaging findings of vascular lesions in the head and neck

Serkan Güneyli, Naim Ceylan, Selen Bayraktaroğlu, Türker Acar, Recep Savaş

ABSTRACT
Vascular lesions of the head and neck include vascular neoplasms, vascular malformations, and hypervascular lesions, derived from nonvascular soft-tissue elements. We retrospectively evaluated magnetic resonance imaging and computed tomography images of vascular lesions located in the head and neck. Twelve patients (seven males, five females) aged 1–68 years (mean age, 35.25 years) were included in this study. Most of the vascular lesions in our study were histologically diagnosed. The lesions were as follows: a hemangioma located in the parotid space (n=1); a hemangioendothelioma located in the parotid space (n=1); a hemangiopericytoma located in the larynx (n=1); a juvenile angiofibroma located in the nasopharynx (n=1); a glomus tumor located in the carotid bifurcation (n=1); venous malformations located in the parapharyngeal space, the pterygoid area, the orbital space, and the larynx (n=4); lymphatic malformations located in the parotid space and the supraclavicular area (n=2); and an arteriovenous malformation located in the infratemporal fossa (n=1). We present rare vascular lesions of the head and neck, which have typical radiological findings.

The International Society for the Study of Vascular Anomalies (ISSVA) classification system provides an approach based on histopathology, clinical course, and treatment (1). The ISSVA classification system divides vascular anomalies into two primary biological categories: vascular neoplasms and vascular malformations. Vascular neoplasms include infantile hemangioma, congenital hemangioma, hemangioendothelioma, tufted angioma, angiosarcoma, and dermatologic acquired vascular neoplasms. Vascular malformations include low-flow malformations (capillary, venous, and lymphatic), high-flow malformations (arterial malformation, arteriovenous malformation, and arteriovenous fistula), and combined malformations (i.e., venolymphatic malformation). Vascular neoplasms have increased endothelial cell turnover (i.e., they proliferate and undergo mitosis), whereas vascular malformations are structural abnormalities of the capillary, venous, lymphatic, and arterial system that grow in proportion to the child (1). There are also lesions, which demonstrate marked neovascularity despite being derived from nonvascular soft-tissue elements. These hypervascular lesions should be distinguished from the vascular endothelial cell-derived neoplasms existing in the ISSVA classification system.

We retrospectively evaluated magnetic resonance imaging (MRI) and computed tomography (CT) images of vascular lesions located in the head and neck, between 2005 and 2008 in our institution. Twelve patients (seven males, five females) aged 1–68 years (mean age, 35.25 years) were included in this study. Informed consent was obtained from all patients. We identified two vascular neoplasms existing in the ISSVA classification sytem: a congenital hemangioma and a hemangioendothelioma. In addition, we identified a hemangiopericytoma, a juvenile angiofibroma, and a glomus tumor, which are hypervascular lesions derived from nonvascular soft-tissue elements. There are four venous malformations, two lymphatic malformations, and an arteriovenous malformation in our study. Most of these vascular lesions were histologically diagnosed. Examinations were performed by a 16-slice CT and a 1.5 Tesla magnetic resonance scanner.

Hemangioma

Hemangioma is a benign lesion consisting of a hamartomatous growth of capillaries with a high proliferation index (2). Hemangioma is the most common vascular neoplasm of the head and neck and may be seen in various localizations (3, 4). The ISSVA classification system divides hemangiomas into two types: infantile hemangiomas and congenital hemangiomas. Infantile hemangiomas present between two weeks to two months of life and undergo a proliferative growth phase until they

From the Department of Radiology (S.G. ✉ serkanguneyli@yahoo.com), Salihli State Hospital, Manisa, Turkey; the Department of Radiology (N.C., S.B., R.S.), Ege University School of Medicine, Izmir, Turkey; the Department of Radiology (T.A.), Mevlana University School of Medicine, Konya, Turkey

reach their full size, whereas congenital hemangiomas are distinguished by being fully formed at birth. There are two types of congenital hemangiomas. Noninvoluting type of congenital hemangioma demonstrates proportional growth without regression, while rapidly involuting type of congenital hemangioma regress completely within two years (1). MRI findings have an important role in the diagnosis of hemangiomas. The hemangioma clearly seems homogeneous hyperintense on T2-weighted MRI, and it is usually isointense when compared to muscle on T1-weighted MRI (Fig. 1). Internal flow voids may be seen on hemangiomas. Hemangiomas show vigorous enhancement after contrast administration (1).

Hemangioendothelioma and hemangiopericytoma

Hemangioendotheliomas are neoplasms of vascular endothelial cells. Hemangiopericytomas are neoplasms, derived from the pericytes, which are localized around vessels. Hemangioendothelioma and hemangiopericytoma are intermediate forms, which may transform to malignancy (5). Imaging descriptions of these lesions are limited, and the appearances are often nonspecific. It is not possible to differentiate between hemangioendothelioma and hemangiopericytoma radiologically. These lesions are generally isointense when compared to muscle on T1-weighted MRI, and they show hyperintense or intermediate signal on T2-weighted MRI. Both lesions show diffuse contrast enhancement

on postcontrast MRI (Fig. 2). CT findings are usually nonspecific, consisting of a soft-tissue mass with attenuation similar to that of muscle, although the mass usually enhances with contrast material (Fig. 3).

Juvenile angiofibroma

Juvenile angiofibroma is a polypoid and locally aggressive lesion, located in the nasal cavity. It is derived from primitive mesenchyme of the sphenopalatine foramen, extending into the pterygopalatine and infratemporal fossa. Juvenile angiofibroma may require an embolization procedure either preoperatively or to stop an acute bleeding (6). MRI demonstrates heterogeneous T1- and T2-weighted signals with vascular flow voids indicating that the lesion is hypervascular (7). In case of bone destruction, CT can show the bone lesions. Juvenile angiofibro-

ma shows diffuse contrast enhancement on postcontrast MRI (Fig. 4).

Glomus tumor

Glomus tumors are hypervascular and benign tumors, classified under three types: glomus vagale is derived from the parapharyngeal region, while glomus jugulare may extend down from an eroded jugular fossa, and glomus caroticum is typically located in the carotid bifurcation (8). Glomus tumors show heterogeneous T1-weighted signal with vascular flow voids, and they are hyperintense on T2-weighted MRI (Fig. 5). These hypervascular lesions show diffuse contrast enhancement on early arterial phase of postcontrast MRI.

Venous malformation

Low-flow vascular malformations include capillary, venous, and lym-
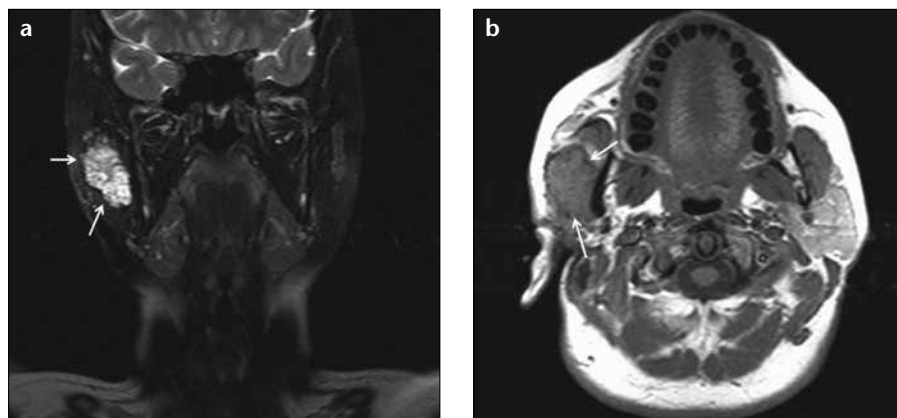
Figure 1. a, b. Fat-saturated T2-weighted coronal MRI **(a)** of a 38-year-old female patient shows a noninvoluting congenital hemangioma appearing as a hyperintense multiseptate lesion *(arrows)* located in the right parotid space. The lesion *(arrows)* is isointense when compared to muscle on T1-weighted axial MRI **(b)** and shows contrast enhancement on postcontrast T1-weighted MRI.
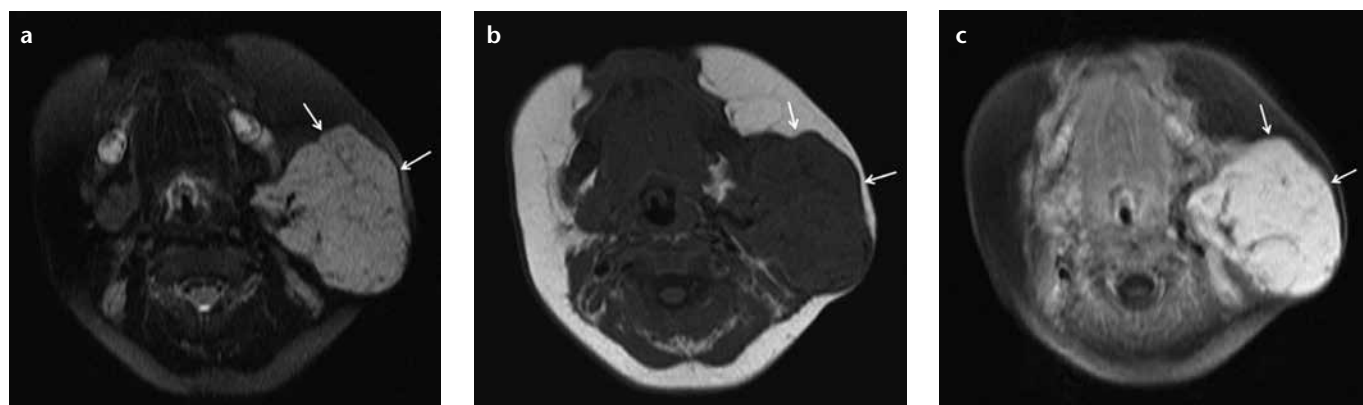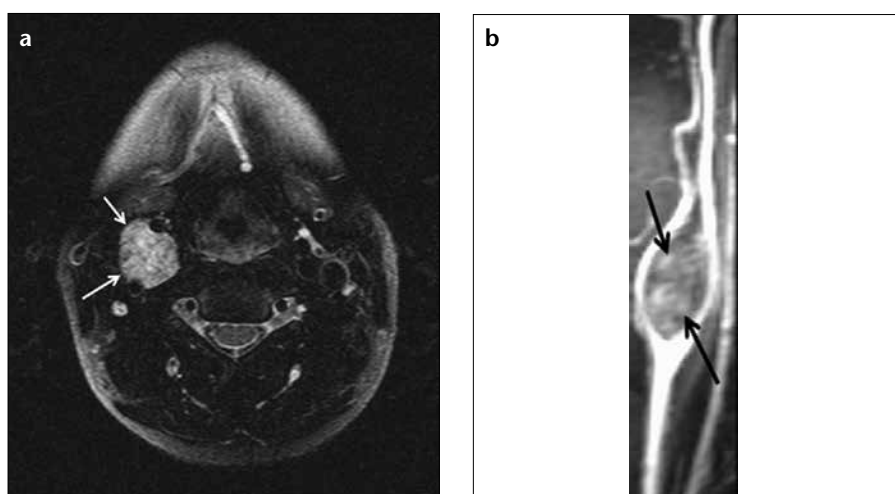

Figure 2. a–c. Fat-saturated T2-weighted axial MRI **(a)** of a 1-year-old female patient shows a large-sized hyperintense hemangioendothelioma *(arrows)* located in the left parotid space. The lesion *(arrows)* is isointense when compared to muscle on T1-weighted axial MRI **(b)** and shows diffuse contrast enhancement on postcontrast fat-saturated T1-weighted axial MRI **(c)**.
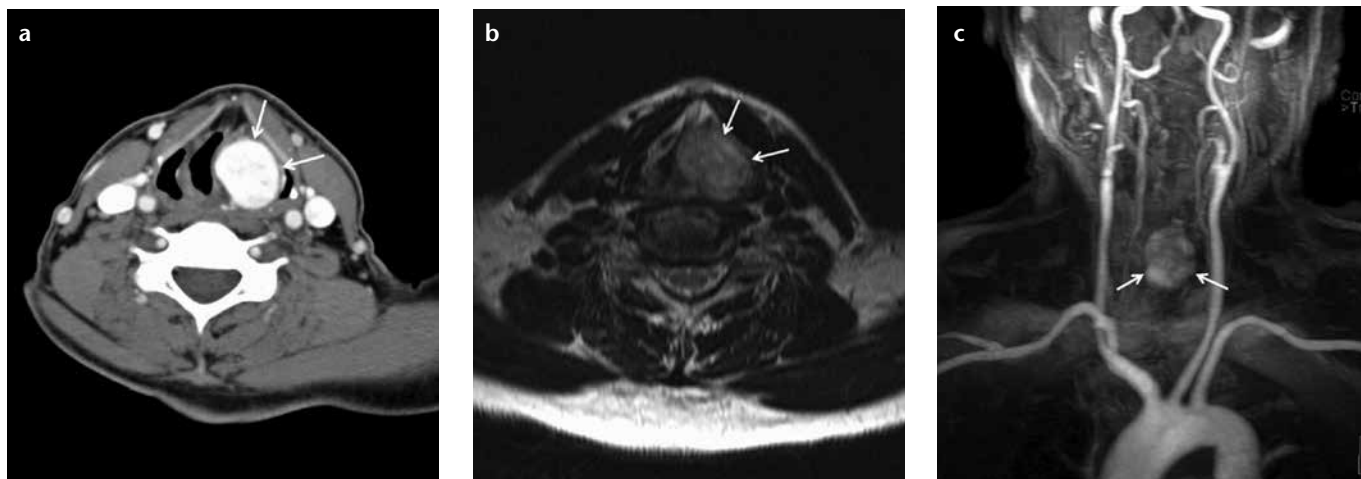
Figure 3. a–c. Axial CT angiography image **(a)** of a 57-year-old male patient shows a regular-shaped hyperdense hemangiopericytoma *(arrows)* narrowing the airway. The lesion is located in the larynx, covering the left paraglottic space. T2-weighted axial MRI **(b)** shows intermediate signal, and postcontrast coronal magnetic resonance (MR) angiography multiplanar reconstruction arterial phase image **(c)** clearly shows the lesion *(arrows)*.
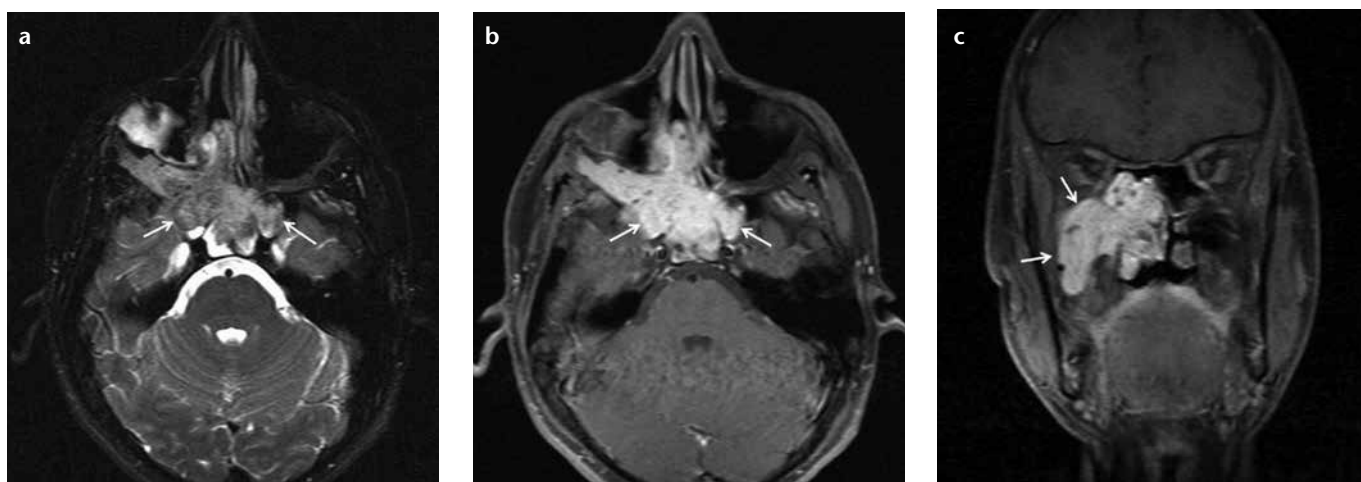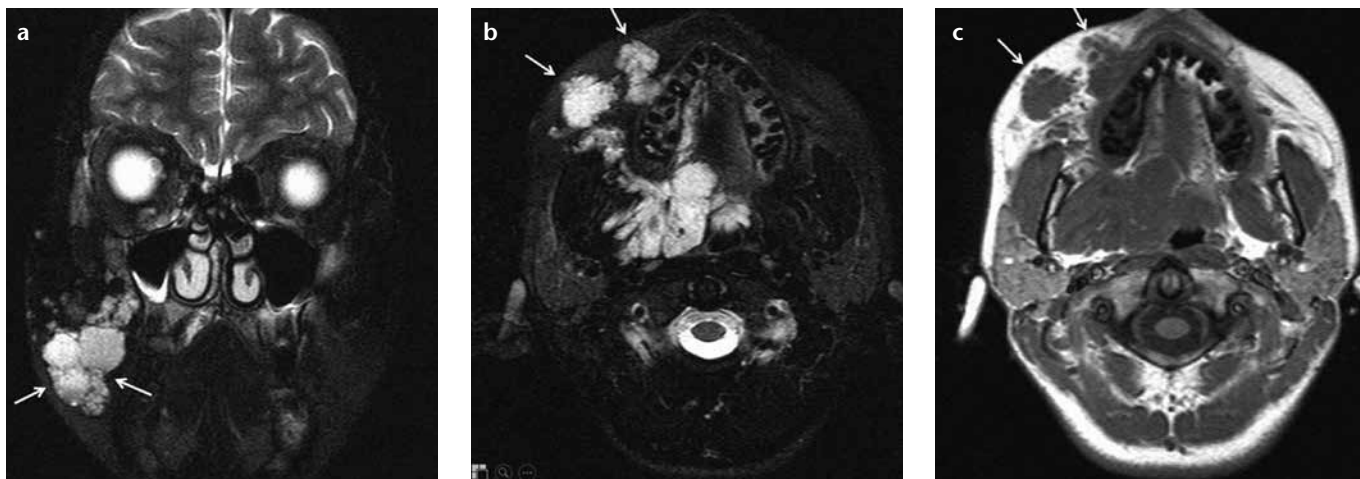

Figure 4. a–c. Fat-saturated T2-weighted axial MRI **(a)** of a 15-year-old male patient shows a nasopharyngeal juvenile angiofibroma *(arrows)* of intermediate signal with invasion of the right pterygopalatine and infratemporal fossa. The lesion *(arrows)* shows diffuse contrast enhancement on postcontrast fat-saturated T1-weighted axial MRI **(b)** and postcontrast fat-saturated T1-weighted coronal MRI **(c)**.
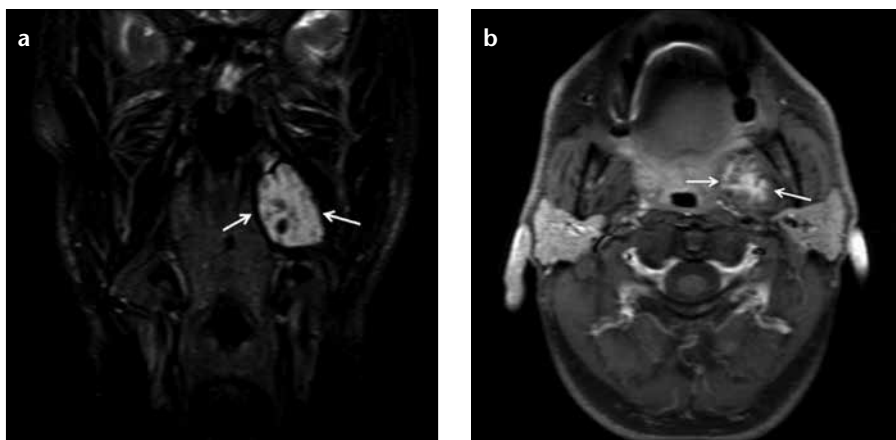

Figure 5. a, b. Fat-saturated T2-weighted axial MRI **(a)** of a 36-year-old female patient shows a hyperintense glomus caroticum *(arrows)*, typically located in the carotid bifurcation. Postcontrast coronal MR angiography arterial phase image **(b)** shows that the hyperintense lesion splays the internal and external carotid arteries symmetrically.

phatic malformations. Venous, lymphatic, and venolymphatic malformations are the most common types of vascular malformations with an overall prevalence of up to 1% in the general population (1). The previously called cavernous hemangiomas of any organ, including hepatic, vertebral, and orbital hemangiomas are actually venous malformations. These venous malformations are non-involuting and may apparently grow in size without proliferative potential (8). Venous malformations appear hyperintense on T2-weighted MRI and may show heterogeneous signal on T1-weighted MRI (Fig. 6). There are no flow voids on MRI. Venous malformations may be tubular, septated,

Figure 6. a–c. Fat-saturated T2-weighted coronal MRI **(a)** of a 17-year-old male patient shows a venous malformation *(arrows)* located in the right parapharyngeal space and the buccal fat pad *(arrows)*. Fat-saturated T2-weighted axial MRI **(b)** shows an irregular-shaped hyperintense lesion *(arrows)*. The lesion *(arrows)* is isointense when compared to muscle on T1-weighted axial MRI **(c)** and shows contrast enhancement on postcontrast T1-weighted axial MRI.

Figure 7. a, b. Fat-saturated T2-weighted coronal MRI **(a)** of a 47-year-old male patient shows a venous malformation *(arrows)* in the left pterygoid area, containing calcification and septa. The lesion *(arrows)* shows contrast enhancement on postcontrast fat-saturated T1-weighted axial MRI **(b)**.
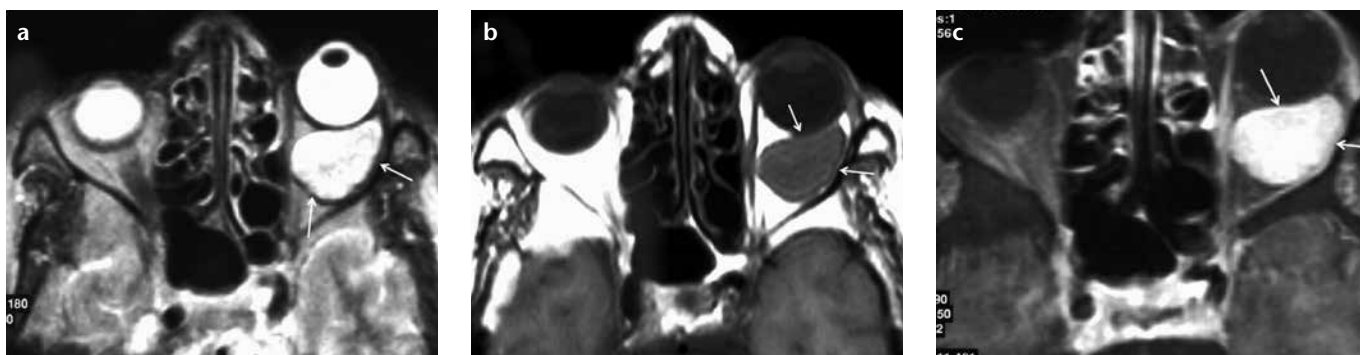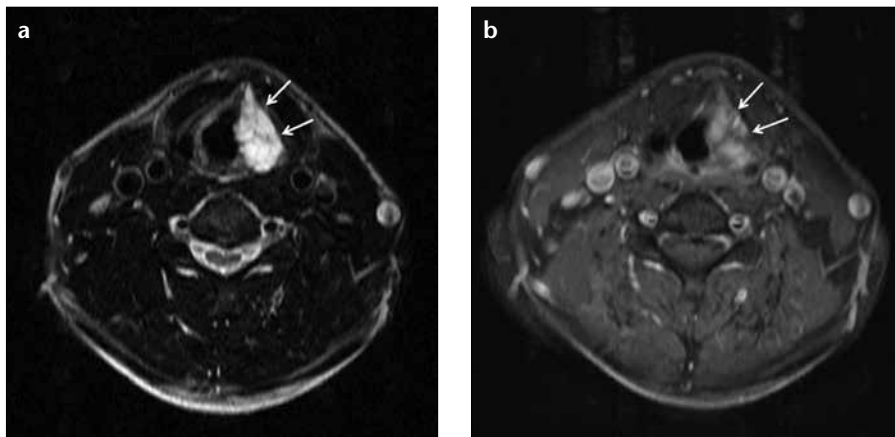

Figure 8. a–c. T2-weighted axial MRI **(a)** of a 68-year-old female patient shows a venous malformation as a septated, hyperintense lesion *(arrows)* located in the intraconal area of the left orbital space. The regular-shaped lesion *(arrows)* is isointense when compared to muscle on T1-weighted axial MRI **(b)** and shows diffuse contrast enhancement on postcontrast fat-saturated T1-weighted axial MRI **(c)**.

and may contain calcification (Fig. 7). The calcifications are hypointense on all MRI sequences and hyperdense on CT. These lesions show significant contrast enhancement on postcontrast MRI (Figs. 8 and 9).

Lymphatic malformation

Lymphatic malformations are most commonly located in the head and neck. The main division in classifying lymphatic malformations is whether they contain macrocysts (>2 cm), mi-

crocysts (<2 cm), or both. Macrocystic lesions are more easily treated and carry a better prognosis than its microcystic counterpart (9). T1-weighted MRI generally shows intermediate or hypointense signal, and the lymphat-

Figure 9. a, b. Fat-saturated T2-weighted axial MRI **(a)** of a 60-year-old male patient shows a hyperintense laryngeal venous malformation *(arrows)* that narrows the airway. The lesion *(arrows)* shows contrast enhancement on postcontrast fat-saturated T1-weighted axial MRI **(b)**.

Figure 10. a–c. Fat-saturated T2-weighted axial MRI **(a)** of a 16-year-old male patient shows a venolymphatic malformation as a septated hyperintense lesion *(arrows)* located in the right parotid space. The lesion *(arrows)* shows heterogeneous signal on fat-saturated T1-weighted axial MRI **(b)**. The lesion *(arrows)* shows peripheral contrast enhancement on postcontrast fat-saturated T1-weighted axial MRI **(c)**.
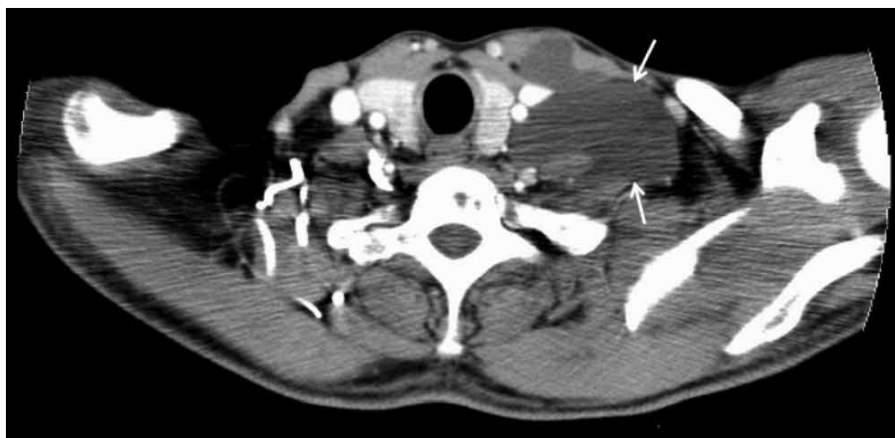
Figure 11. Postcontrast axial CT image of a 51-year-old male patient shows a left supraclavicular lymphatic malformation appearing as a regular-shaped hypodense lesion *(arrows)*.

ic malformations are mostly hyperintense on T2-weighted MRI. Lymphatic malformations may be septated. Hemorrhagic lymphatic malformations may be called as venolymphatic malformations (Fig. 10). Lympatic malformations usually do not show contrast enhancement on postcontrast MRI and CT images (Fig. 11).

Arteriovenous malformation

High-flow vascular malformations include arterial malformations, arteriovenous malformations, and arteriovenous fistulae. Abnormal connections are seen between the arterial and venous systems due to abnormality at the capillary level on the arteriovenous malformations and fistulae (10). Arteriovenous malformations demonstrate a nidus of small vessels between the arteries and draining vein, whereas a fistula is composed of a macroscopic arteriovenous connection. The treatment for arteriovenous malformation should aim to eradicate the nidus completely, otherwise residual nidus would give rise to a recurrence (11). CT and MRI classically demonstrate enlarged vascular channels without an associated soft-tissue mass, but there may be perilesional T2-weighted hyperintensity due to edema and venous congestion or a fibrofatty matrix (12). This appearance should not be confused with a vascular neoplasm. Postcontrast CT and MRI clearly show the arterial and venous tubular vascular components (Fig. 12).
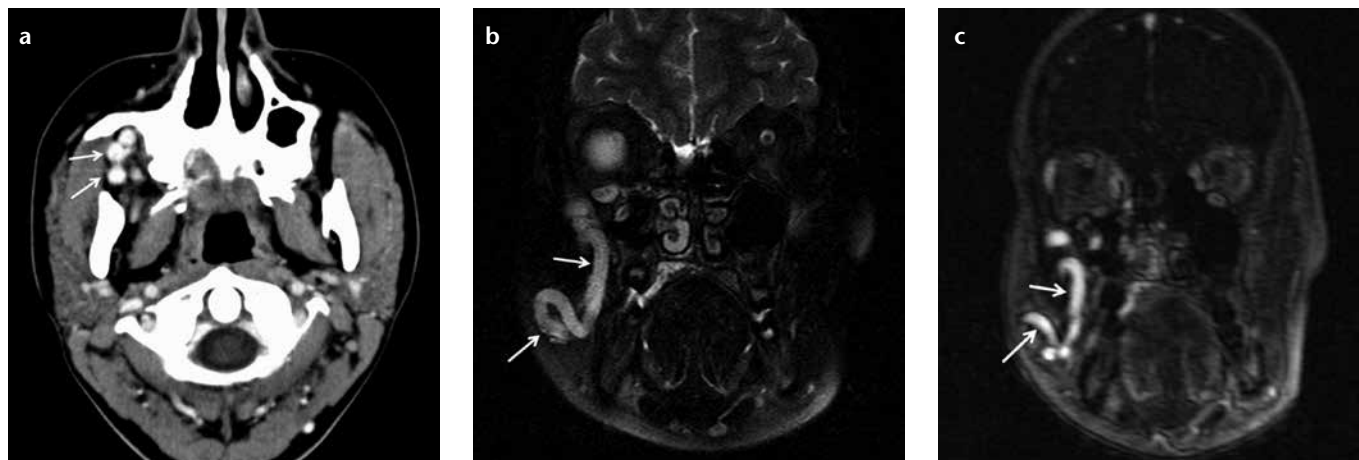
Figure 12. a–c. Postcontrast axial CT image **(a)** of a 17-year-old female patient shows a hyperdense arteriovenous malformation *(arrows)* located in the right infratemporal fossa. Fat-saturated T2-weighted coronal MRI **(b)** shows the dilated vascular structure *(arrows)*. Postcontrast coronal MR angiography arterial phase image **(c)** shows the hyperintense arterial and venous dilated vascular components *(arrows)*.

Conclusion

We presented 12 rare and exemplary vascular lesions with their appearances on CT and MRI. Biopsy for the diagnosis of the vascular lesions located in the head and neck is occasionally difficult and risky, because of complications such as hemorrhage. These vascular lesions may be diagnosed by their typical imaging findings (8, 13, 14). Additionally, radiology has a role in showing the extent of lesions, which is important for therapy and follow-up.

Conflict of interest disclosure

The authors declared no conflicts of interest.

References

1. Lowe LH, Marchant TC, Rivard DC, Scherbel AJ. Vascular malformations: classification and terminology the radiologist needs to know. Semin Roentgenol 2012; 47:106–117. **[CrossRef]**

2. Donnelly LF, Adams DM, Bisset GS. Vascular malformations and hemangiomas: a practical approach in a multidisciplinary clinic. AJR Am J Roentgenol 2000; 174:597–608. **[CrossRef]**

3. Sundine MJ, Wirth GA. Hemangiomas: An overview. Clin Pediatr 2007; 46:206–221. **[CrossRef]**

4. Stal S, Hamilton S, Spira M. Hemangiomas, lymphangiomas, and vascular malformations of the head and neck. Otolaryngol Clin North Am 1986; 19:769–796.

5. Murphey MD, Fairbairn KJ, Parman LM, Baxter KG, Parsa MB, Smith WS. Musculoskeletal angiomatous lesions: radiologic-pathologic correlation. Radiographics 1995; 15:893–917. **[CrossRef]**

6. Kulkarni SS, Shetty NS, Dharia TP, Polnaya AM. Pictorial Essay: Vascular interventions in extra cranial head and neck. Indian J Radiol Imaging 2012; 22:350–357. **[CrossRef]**

7. Lloyd G, Howard D, Lund V, Savy L. Imaging for juvenile angiofibroma. J Laryngol Otol 2000; 114:727–730. **[CrossRef]**

8. Connor SEJ, Flis C, Langdon JD. Vascular masses of the head and neck. Clin Radiol 2005; 60: 856–868. **[CrossRef]**

9. Buckmiller LM, Richter GT, Suen JY. Diagnosis and management of hemangiomas and vascular malformations of the head and neck. Oral Dis 2010; 16:405–418. **[CrossRef]**

10. Burrows PE, Lao T, Paltiel H, Robertson RL. Diagnostic imaging in the evaluation of vascular birthmarks. Dermatol Clin 1998; 16:455–488. **[CrossRef]**

11. Kohout MP, Hansen M, Pribaz JJ, Mulliken JB. Arteriovenous malformations of the head and neck: natural history and management. Plast Reconstr Surg 1998; 102:643–654. **[CrossRef]**

12. Meyer JS, Hoffer FA, Barnes PD, Mulliken JB. Biological classification of soft-tissue vascular anomalies: MR correlation. AJR Am J Roentgenol 1991; 157:559–564. **[CrossRef]**

13. Kakimato N, Tanimoto K, Nishiyama H, Murakami S, Furukawa S, Kreiborg S. CT and MR imaging features of oral and maxillofacial hemangioma and vascular malformation. Eur J Radiol 2005; 55:108–112. **[CrossRef]**

14. Fordham LN, Chung CJ, Donnelly LF. Imaging of congenital vascular and lymphatic anomalies of the head and neck. Neuroimaging Clin N Am 2000; 10:117–136.